

Novel $\text{ReBaCo}_{1.5}\text{Mn}_{0.5}\text{O}_{5+\delta}$ (Re: La, Pr, Nd, Sm, Gd and Y) perovskite oxides: influence of manganese doping on crystal structure, oxygen nonstoichiometry, thermal expansion, transport properties, and application as cathode materials in Solid Oxide Fuel Cells

Anna Olszewska^a, Zhihong Du^b, Konrad Świerczek^{a,c#}, Hailei Zhao^{b,d*}, Bogdan Dabrowski^e

^aAGH University of Science and Technology, Faculty of Energy and Fuels,
al. A. Mickiewicza 30, 30-059 Krakow, Poland

^bUniversity of Science and Technology Beijing, School of Materials Science and Engineering,
Beijing 100083, China

^cAGH Centre of Energy, AGH University of Science and Technology,
ul. Czarnowiejska 36, 30-054 Krakow, Poland

^dBeijing Municipale Key Lab for Advanced Energy Materials and Technologies,
Beijing 100083, China

^eDepartment of Physics, Northern Illinois University, DeKalb, Illinois 60115, USA

#xi@agh.edu.pl

*hlzhao@ustb.edu.cn

Supplementary Information

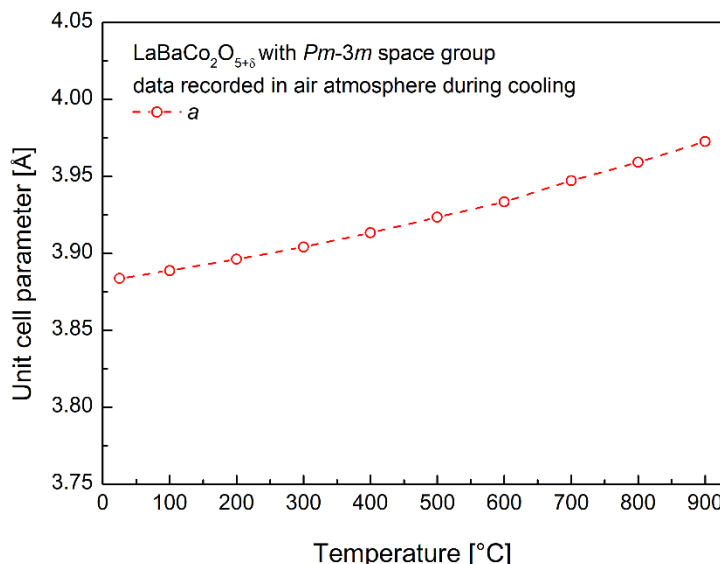


Fig. S1a. Temperature dependence of the unit cell parameter for $\text{LaBaCo}_2\text{O}_{5+\delta}$.

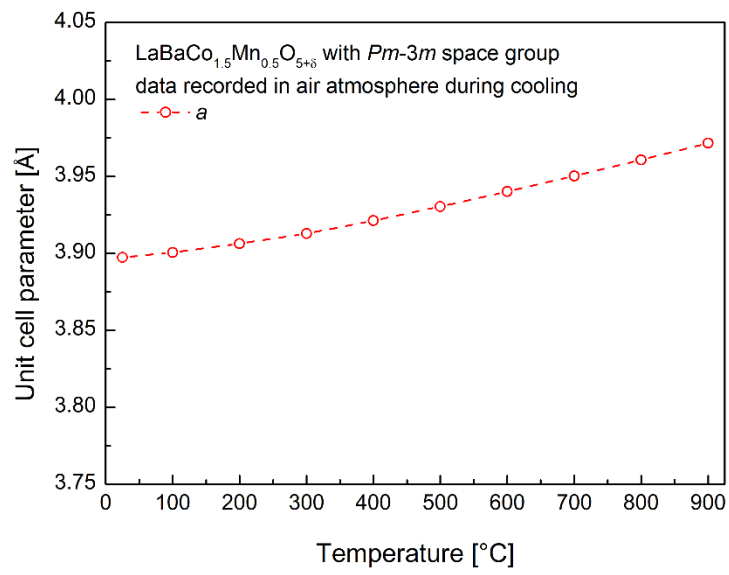


Fig. S1b. Temperature dependence of the unit cell parameter for $\text{LaBaCo}_{1.5}\text{Mn}_{0.5}\text{O}_{5+\delta}$.

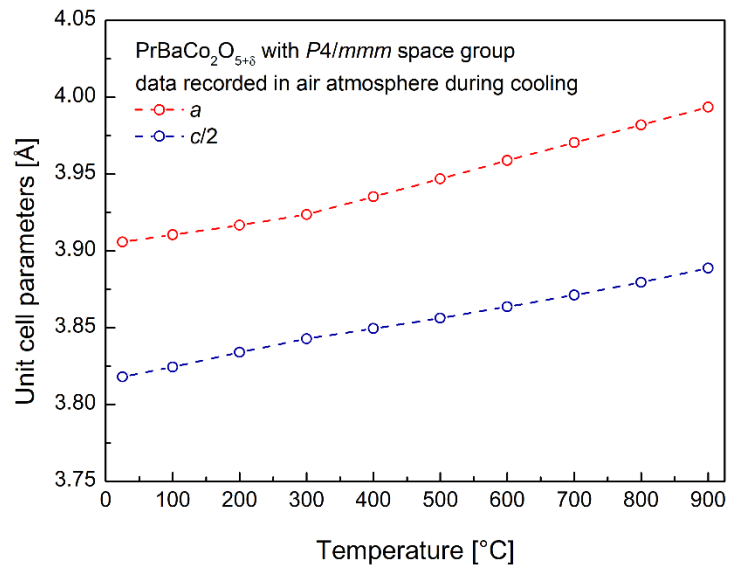


Fig. S2a. Temperature dependence of the unit cell parameters for $\text{PrBaCo}_2\text{O}_{5+\delta}$.

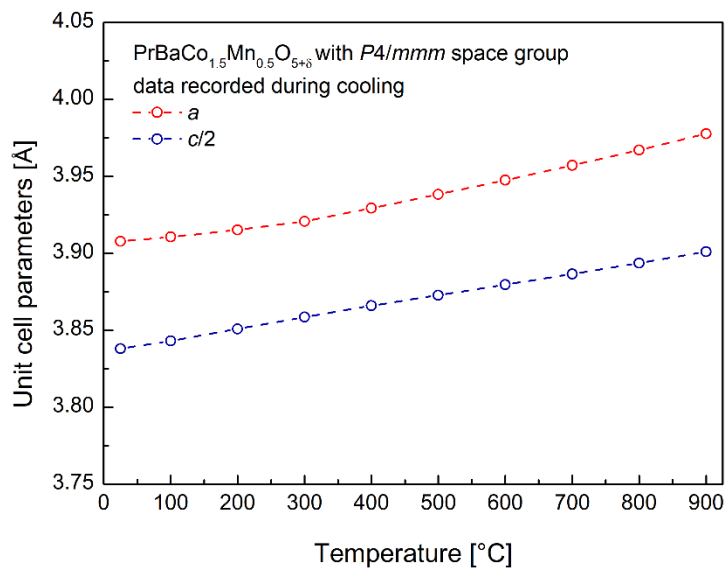


Fig. S2b. Temperature dependence of the unit cell parameters for Pr_{0.5}BaCo_{1.5}Mn_{0.5}O_{5+δ}.

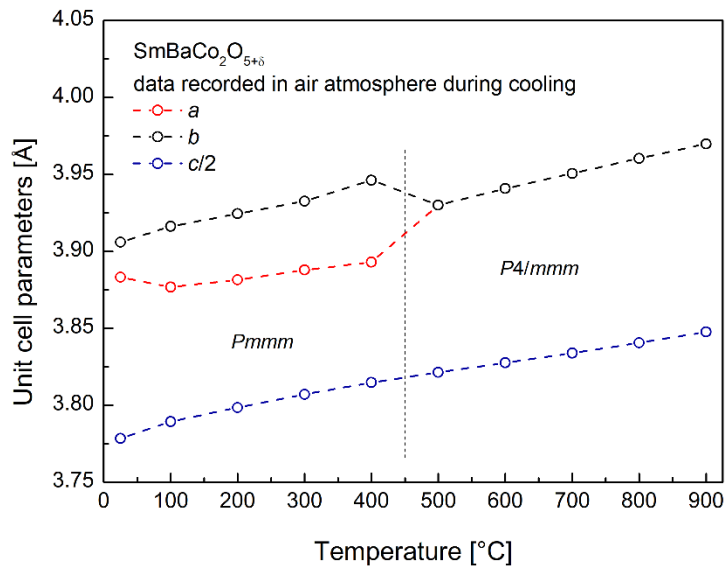


Fig. S3a. Temperature dependence of the unit cell parameters for SmBaCo₂O_{5+δ}.

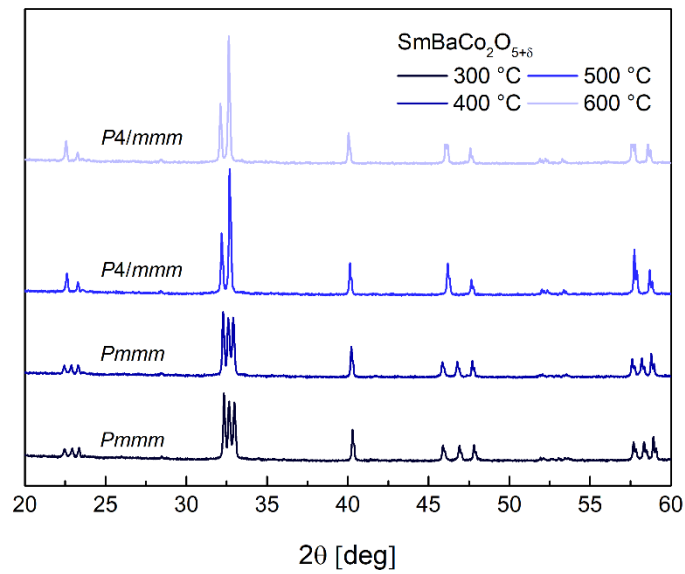


Fig. S3b. Selected range of XRD data for $\text{SmBaCo}_2\text{O}_{5+\delta}$ recorded at different temperatures.

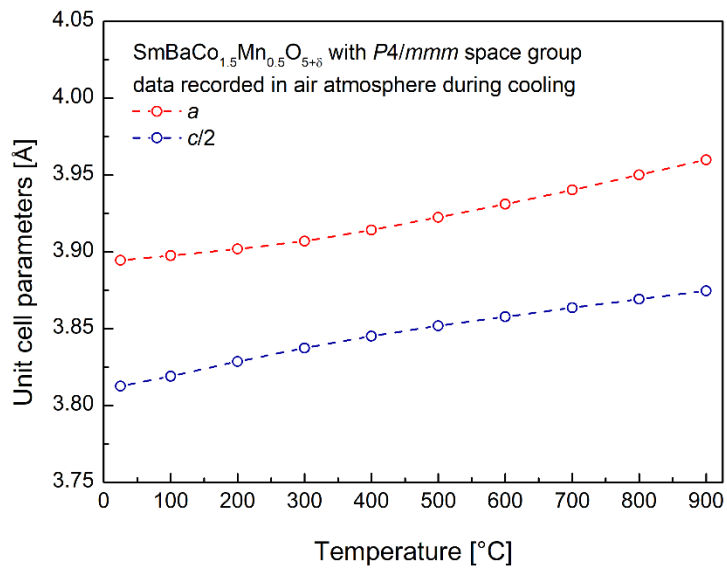


Fig. S3c. Temperature dependence of the unit cell parameters for $\text{SmBaCo}_{1.5}\text{Mn}_{0.5}\text{O}_{5+\delta}$.

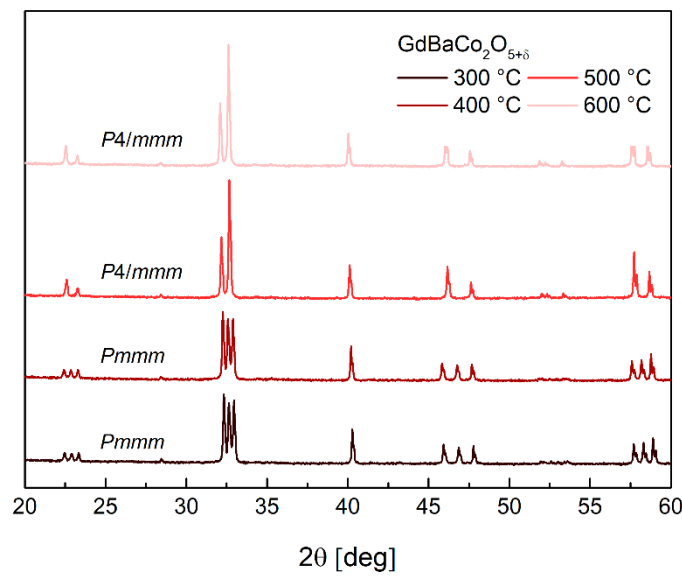


Fig. S4. Selected range of XRD data for $\text{GdBaCo}_2\text{O}_{5+\delta}$ recorded at different temperatures.

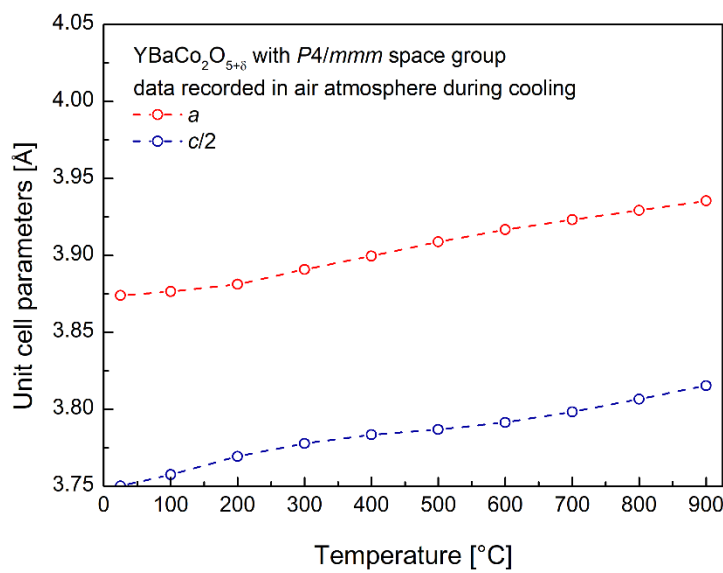


Fig. S5a. Temperature dependence of the unit cell parameters for $\text{YBaCo}_2\text{O}_{5+\delta}$.

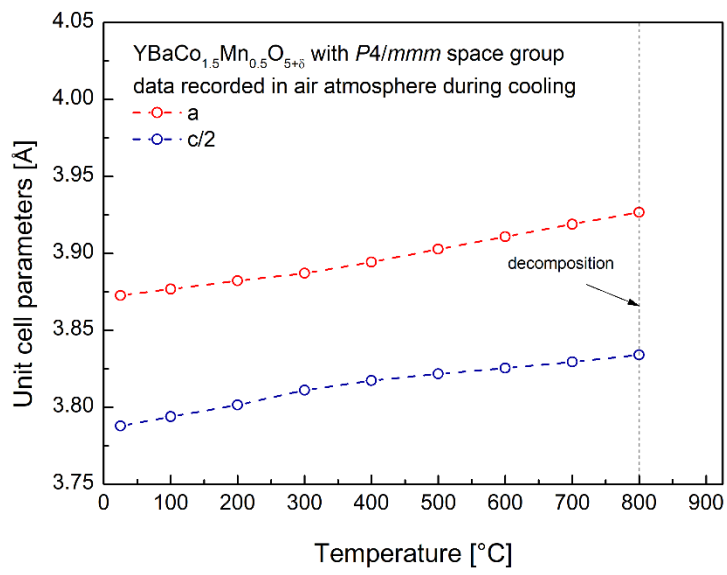


Fig. S5b. Temperature dependence of the unit cell parameters for YBaCo_{1.5}Mn_{0.5}O_{5+δ}.

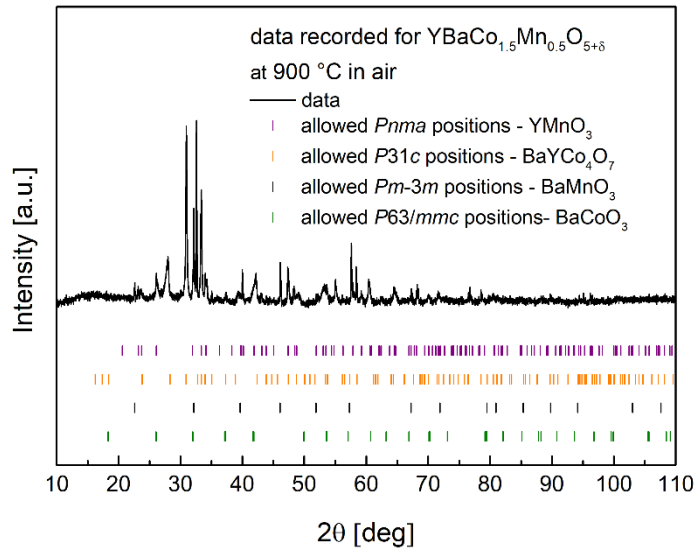


Fig. S5c. Decomposition of YBaCo_{1.5}Mn_{0.5}O_{5+δ} as visible in HT-XRD measurement at 900 °C.

Tab. S1. Values of the oxygen content, calculated for 600, 700, 800 and 900 °C for ReBaCo₂O_{5+δ} and ReBaCo_{1.5}Mn_{0.5}O_{5+δ} oxides (± 0.01).

	600 °C	700 °C	800 °C	900 °C
ReBaCo₂O_{5+δ}				
La	5.74	5.67	5.61	5.54
Pr	5.55	5.49	5.43	5.36
Nd	5.51	5.45	5.39	5.33
Sm	5.43	5.37	5.30	5.25
Gd	5.33	5.25	5.18	5.12
Y	5.06	5.02	4.99	4.99
ReBaCo_{1.5}Mn_{0.5}O_{5+δ}				
La	5.84	5.79	5.74	5.69
Pr	5.74	5.70	5.65	5.60
Nd	5.71	5.67	5.62	5.57
Sm	5.62	5.57	5.51	5.46
Gd	5.54	5.49	5.43	5.38
Y	5.40	5.33	5.27	5.25

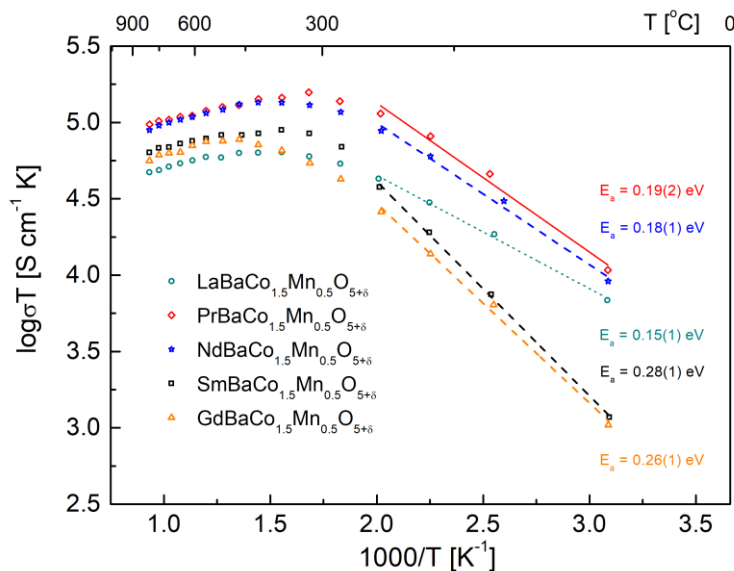


Fig. S6. Arrhenius-type plot used to calculate activation energy of the electrical conductivity of ReBaCo_{1.5}Mn_{0.5}O_{5+δ}. E_a was estimated in 50-200 °C range.

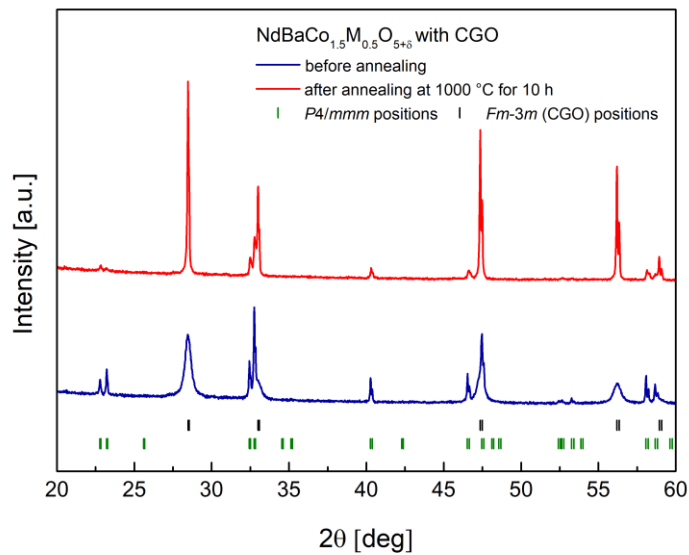


Fig. S7a. XRD patterns recorded for $\text{NdBaCo}_{1.5}\text{Mn}_{0.5}\text{O}_{5+\delta}$ mixed with CGO, before and after annealing at 1000 °C. Please notice that CGO-related peaks become very narrow after heat treatment.

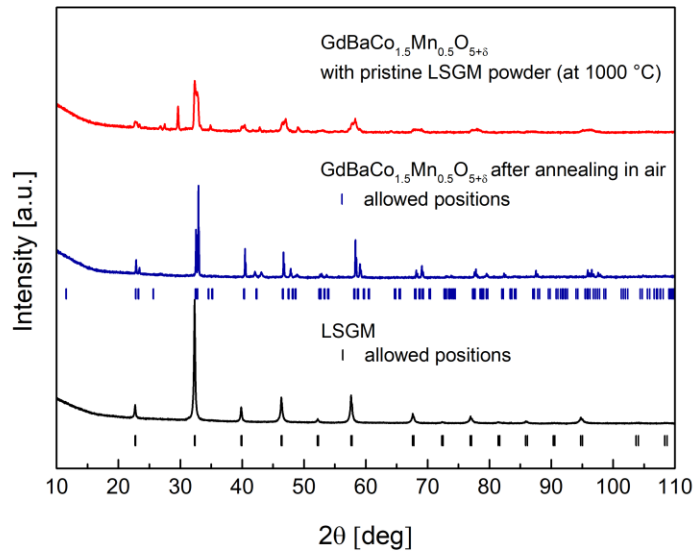


Fig. S7b. XRD studies of $\text{GdBaCo}_{1.5}\text{Mn}_{0.5}\text{O}_{5+\delta}$ stability in relation to LSGM electrolyte.

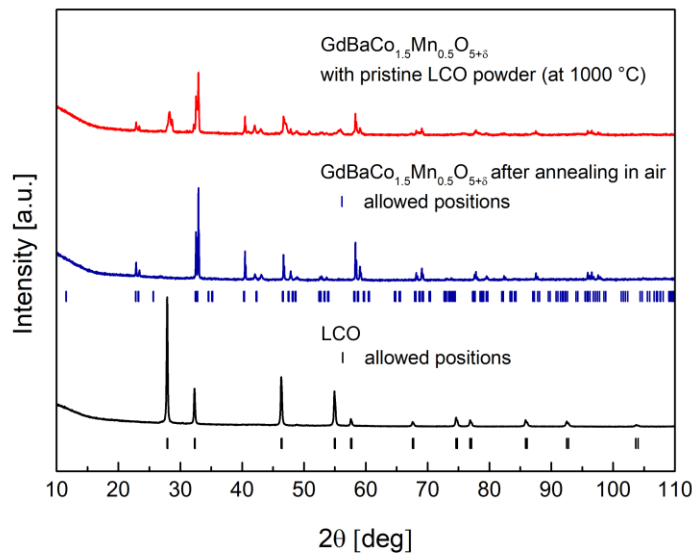


Fig. S7c. XRD studies of GdBaCo_{1.5}Mn_{0.5}O_{5+δ} stability in relation to LCO electrolyte.

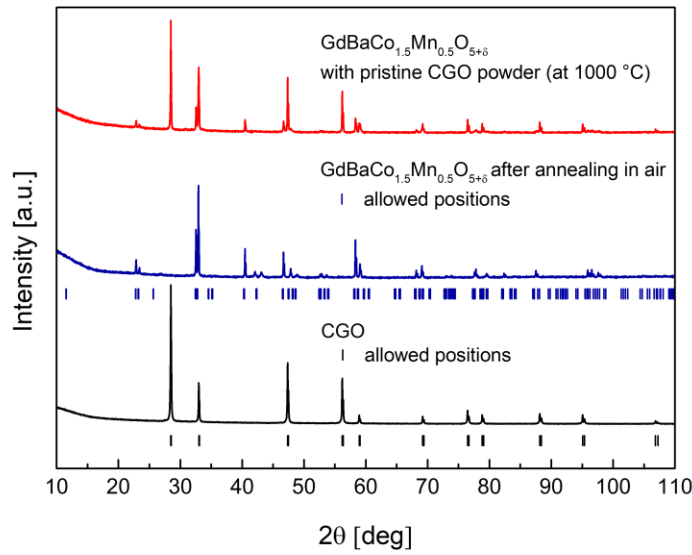


Fig. S7d. XRD studies of GdBaCo_{1.5}Mn_{0.5}O_{5+δ} stability in relation to CGO electrolyte.

Tab. S2. Refined values of the unit cell parameters and FWHM of the main perovskite peak for $\text{NdBaCo}_{1.5}\text{Mn}_{0.5}\text{O}_{5+\delta}$ and $\text{GdBaCo}_{1.5}\text{Mn}_{0.5}\text{O}_{5+\delta}$ oxides after stability tests with pristine LSGM, LCO and CGO electrolytes.

	<i>a</i> parameter [Å]	<i>c</i> parameter [Å]	FWHM [deg]
NdBaCo_{1.5}Mn_{0.5}O_{5+δ}			
1000 °C, air	3.9003(1)	7.6562(1)	0.075
+ LSGM (1000 °C)	3.8469(1)	7.6852(1)	0.339
+ LCO (1000 °C)	3.9018(1)	7.6595(1)	0.104
+ CGO (1000 °C)	3.8977(1)	7.6592(1)	0.124
+ CGO (1100 °C)	3.8942(1)	7.6508(1)	0.172
+ CGO (1200 °C)	3.8954(1)	7.6550(1)	0.162
GdBaCo_{1.5}Mn_{0.5}O_{5+δ}			
1000 °C, air	3.8877(1)	7.5996(1)	0.075
+ LSGM (1000 °C)	3.8746(1)	7.7209(1)	0.473
+ LCO (1000 °C)	3.8879(1)	7.6063(1)	0.117
+ CGO (1000 °C)	3.8862(1)	7.6010(1)	0.116
+ CGO (1100 °C)	3.8882(1)	7.6013(1)	0.154
+ CGO (1200 °C)	3.8900(1)	7.5989(1)	0.152

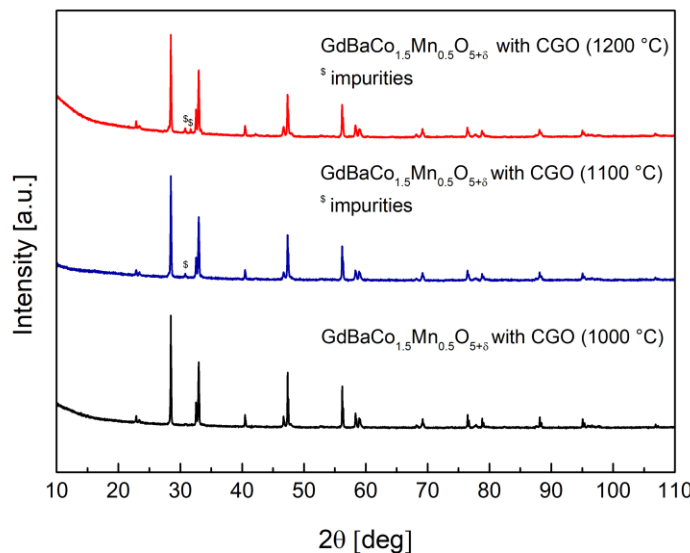


Fig. S8. XRD studies of $\text{GdBaCo}_{1.5}\text{Mn}_{0.5}\text{O}_{5+\delta}$ stability in relation to CGO electrolyte at different temperatures.

Tab. S3. Values of cathodic polarization R_p as a function of temperature determined for symmetrical cells with $\text{NdBaCo}_{1.5}\text{Mn}_{0.5}\text{O}_{5+\delta}$ cathode layers synthesized at different temperatures and sintered in 1000-1200 °C range.

sintering temperature		measurement temperature		
[°C]		[°C]		[°C]
	800	850	900	
synthesized at 1200 °C			R_p [Ω cm²]	
1000	1.556	0.848	0.409	
1100	0.346	0.206	0.122	
1200	5.248	2.235	1.017	
synthesized at 1000 °C			R_p [Ω cm²]	
1050	0.420	0.238	0.139	
1075	0.372	0.202	0.112	
1100	0.117	0.070	0.043	
1125	0.387	0.234	0.141	

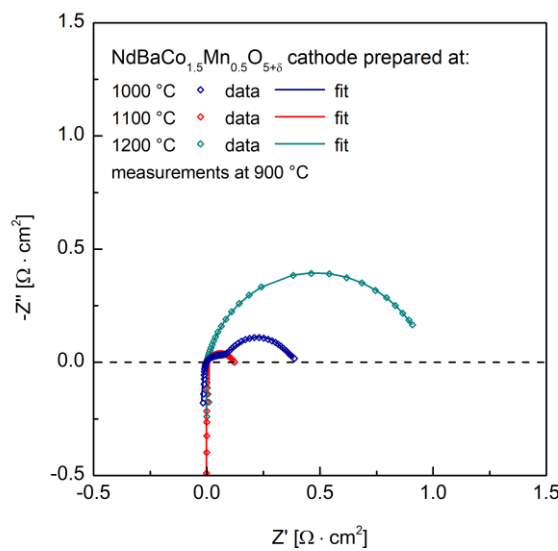


Fig. S9. Measured impedance data for symmetrical cells with $\text{NdBaCo}_{1.5}\text{Mn}_{0.5}\text{O}_{5+\delta}$ cathode synthesized at 1200 °C and prepared at different temperatures. Ohmic resistance was subtracted and the values were divided by two, due to the symmetric configuration, which allowed to estimate cathodic polarization R_p .